The Journal of Chemical Physics

Quantum coherent control of H_3^+ formation in strong fields

Cite as: J. Chem. Phys. **150**, 044303 (2019); https://doi.org/10.1063/1.5070067
Submitted: 18 October 2018 . Accepted: 18 December 2018 . Published Online: 23 January 2019

Matthew J. Michie, Nagitha Ekanayake, Nicholas P. Weingartz, Jacob Stamm, and Marcos Dantus

The Journal of Chemical Physics ARTICLE scitation.org/journal/jcp

Quantum coherent control of H_3^+ formation in strong fields

Cite as: J. Chem. Phys. 150, 044303 (2019); doi: 10.1063/1.5070067
Submitted: 18 October 2018 • Accepted: 18 December 2018 •
Published Online: 23 January 2019

Matthew J. Michie, Nagitha Ekanayake, Nicholas P. Weingartz, Jacob Stamm, and Marcos Dantus[1,2,a)]

AFFILIATIONS

[1] Department of Chemistry, Michigan State University, East Lansing, Michigan 48824, USA
[2] Department of Physics and Astronomy, Michigan State University, East Lansing, Michigan 48824, USA

[a)] **Author to whom correspondence should be addressed:** dantus@chemistry.msu.edu

ABSTRACT

Quantum coherent control (QCC) has been successfully demonstrated experimentally and theoretically for two- and three-photon optical excitation of atoms and molecules. Here, we explore QCC using spectral phase functions with a single spectral phase step for controlling the yield of H_3^+ from methanol under strong laser field excitation. We observe a significant and systematic enhanced production of H_3^+ when a negative $^3/_4\,\pi$ phase step is applied near the low energy region of the laser spectrum and when a positive $^3/_4\,\pi$ phase step is applied near the high energy region of the laser spectrum. In some cases, most notably the HCO^+ fragment, we found the enhancement exceeded the yield measured for transform limited pulses. The observation of enhanced yield is surprising and far from the QCC prediction of yield suppression. The observed QCC enhancement implies an underlying strong field process responsible for polyatomic fragmentation controllable by easy to reproduce shaped pulses.

I. INTRODUCTION

Quantum coherent control (QCC) of two-photon transitions in atoms, illustrated in Fig. 1(a), was elegantly demonstrated by the use of a π-step spectral phase function.[1] Inspiration for their work originated from Brumer and Shapiro who realized that quantum interference, between two pathways, exciting molecular transitions can be manipulated by changing the phase of one or more pathways,[2] as well as the use of pulse shaping to control chemical reactions.[3,4] The designation QCC was made to differentiate the use of a well-defined phase function such as a phase step or sinusoidal function instead of experimental search for a feedback optimized field, which adopts the more generic term, coherent control. When the frequency at which the π step coincides with a two-photon resonance, a constructive quantum interference was predicted and observed in the transition probability; whereas, when the π-step was detuned from the resonance, the transition probability approached zero.[1] The reason for the observed QCC feature was explained by Meshulach and Silberberg using perturbation theory. In their formulation, all quantum mechanical paths leading to the two-photon resonance are integrated [Eq. (1)],

$$\begin{aligned} S_2 &= \left| \int_{-\infty}^{\infty} \epsilon^2(t) \exp(i\omega_0 t) dt \right|^2 \\ &= \left| \int_{-\infty}^{\infty} \bar{\epsilon}(\omega_0/2+\Omega)\bar{\epsilon}(\omega_0/2-\Omega) d\Omega \right|^2 \\ &= \left| \int_{-\infty}^{\infty} A(\omega_0/2+\Omega)A(\omega_0/2-\Omega) \exp[i\{\phi(\omega_0/2+\Omega) \right. \\ &\quad \left. + \phi(\omega_0/2-\Omega)\}] d\Omega \right|^2, \end{aligned} \tag{1}$$

where $A(\omega)$ and $\phi(\omega)$ are the frequency dependent amplitude of the field and the spectral phase of the pulse, respectively. The formula sums the phase for the high- and low-energy detuned photons, for every path. The trivial case being transform limited (TL) pulses, when all photons have a phase of 0 or π, the exponential term for each path becomes e^{i0} or $e^{i2\pi}$,

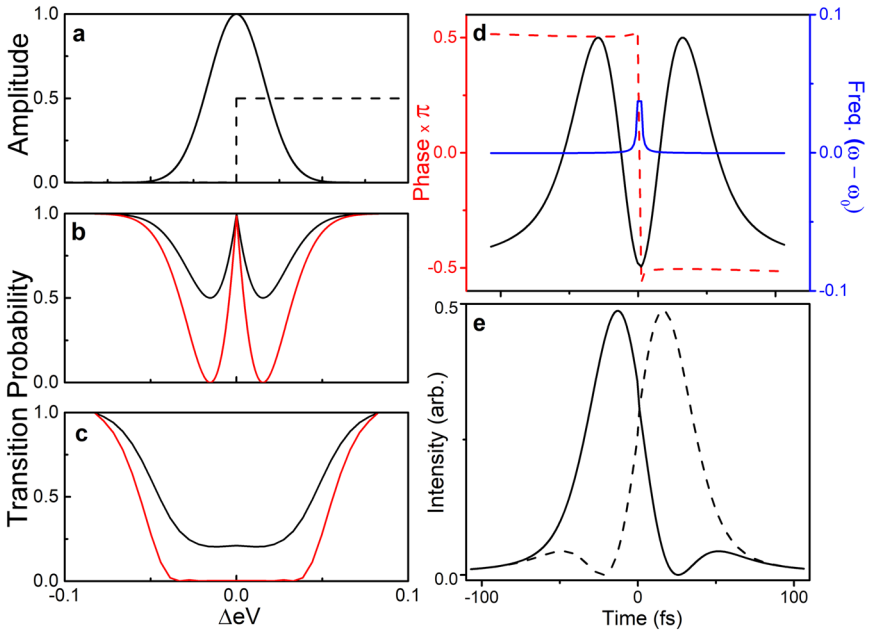

FIG. 1. (a) The spectrum of the pulse (solid) with a $\pi/2$ phase step (dashed). (b) Calculated quantum coherence control (QCC) for a two-photon transition as a function of detuning of the position of a π (red) of $\pi/2$ (black) step. Notice that when the position of the step coincides with the two-photon resonance (0.0 eV detuning), a maximum two-photon transition is observed. (c) Calculated QCC for a 7-photon transition as a function of detuning of the position of a π (red) of $\pi/2$ (black) step. While there are some modulations, there is no significant QCC feature observed. (d) Time-domain representation of a pulse with a π-step in its spectral phase at its carrier frequency. The dotted red line represents the phase with respect to time, $\varphi(t)$, the solid blue line represents the instantaneous frequency, $\omega(t)$, with respect to its carrier frequency, and the solid black line represents the intensity, $I(t)$. (e) Time-domain representation of a pulse with a $\pi/2$ step in its spectral phase at its carrier. The solid black line is the resulting pulse after a negative $\pi/2$ step, while the dashed line shows the resulting pulse after a positive $\pi/2$ step. The phase difference between the two portions of the pulse is π, and the instantaneous frequency is unchanged (not shown) similar to the π step case.

which equals 1. The non-trivial QCC interference occurs when the phase step coincides with a two-photon resonant transition, such that one-half of the frequencies have a phase of 0 and the corresponding half of the frequencies have a phase of π. In that case, the phase dependent term is $e^{i\pi} = -1$ for all of the excitation paths. The absolute value squared makes the result independent of the sign of the phase step. Destructive interference occurs when half of the paths have a phase of 0 and the other half a phase of π. In that case, the two-photon excitation probability approaches 0.

Strong-field laser-matter interactions are well understood for isolated atoms and diatomic molecules, yet our understanding falls short when polyatomic molecules are involved. Similarly, QCC of laser-matter interactions is well known for two- and three-photon resonant transitions, but not understood in cases with higher order transitions. Here, we consider exploring the simplest approach to QCC on a chemical process requiring strong-field double ionization. The goal is to determine if one can use QCC in strong-field laser-matter interactions involving higher order, 7- to 20-photon, excitation.

QCC has been used to control two- and three-photon transitions in atoms and molecules in the gas phase[5] and in the condensed phase.[6] When the phase step is only $\pi/2$, one finds that the magnitude of the QCC is half of that observed for the π-step, noting that there is no difference if the step is positive or negative [Fig. 1(b)]. The coherent resonance condition found for two-photon excitation is replaced by smaller modulations for two- and three-photon transitions.[4] Here, we calculated the case for a seven-photon resonance transition, shown in Fig. 1(c), requiring six integrals that consider every possible pathway and observe that the clear QCC feature is replaced by very shallow modulations that are barely visible. The dominant result in higher order ($n > 4$) transitions is a significant reduction in the transition probability.[7]

A positive or negative π-step at the central frequency of the pulse causes the pulse to break into two parts of equal intensity, with a temporal phase change of π between the two, highlighted by the red dashed line in Fig. 1(d). Interestingly, for the case of a $\pi/2$ spectral phase modulation applied in the center of the spectrum, there is a clear difference between a positive and negative step, as shown in Fig. 1(e).

In the single ionization intensity regime, the resulting molecular ion has relatively low internal energy of excitation, and coherent vibrational motion has been recorded due to differences between the ground state geometry of the neutral species compared to the ground state structure of the ion.[8,9] The subsequent fragmentation of the resulting ion is then dominated by ion stability and the probability of the ion to absorb one or more additional photons to reach

dissociative states.[10] Under the conditions of double ionization, polyatomic organic molecules dissociate into a variety of fragments that range from the molecular ion to hydrogen and carbon atoms. This regime results in a large number of fragment ions, and their relative yield has defied a satisfactory explanation. On one hand, one may consider a molecule under such strong-field to behave as a "bag of atoms" for which there is little or no control and all statistically possible fragment ions are produced. On the other hand, the molecular structure and properties of the laser field may determine the dissociation into multiple fragments, implying that one can shape the field in order to exert control over the yield of different fragment ions.

Previous work on π-step QCC has focused on two- and three-photon absorption in atoms and diatomic molecules.[1,5,11–13] Here, we attempt QCC on the strong-field double-ionization of methanol, and, in particular, the formation of H_3^+ which has received considerable attention.[14–16] The production of H_3^+ proceeds via a mechanism that stems from the formation of a neutral H_2 molecule, which subsequently roams and extracts a proton.[17] The complex mechanism for this reaction requiring the dissociation of three bonds and the creation of three new ones represents an interesting challenge for QCC. Details about the mechanism together with *ab initio* molecular dynamics simulations for the production of H_3^+ from methanol, longer-chain alcohols, and thiols are discussed elsewhere.[17–19]

II. EXPERIMENTAL AND *AB INITIO* CALCULATIONS

A detailed description of the experimental setup used for the experiments is given in the supplementary material. Briefly, an 800-nm fs laser interacts with methanol molecules at 10^{-6} Torr, and ions are detected at right angles by a time-of-flight (ToF) mass spectrometer. The maximum peak intensity of the light is 4.3×10^{14} W/cm^2 (accurate within a factor of 2) and is polarized parallel to the time-of-flight axis. The recorded mass spectrum for methanol under these conditions can be found in the supplementary material. High-order dispersion correction and pulse shaping was carried out using a multiphoton intrapulse interference phase scan (MIIPS) enabled pulse shaper (MIIPS HD, Biophotonic Solutions, Inc.).[20,21] Spectral phase masks were applied to the pulse by the two-dimensional (600 × 800) pixel spatial light modulator (SLM) and consisted of a variation of different π steps with different magnitudes and signs that were scanned across the spectrum of the laser pulse.

To ensure that the induced phase step did not affect the laser focus (position and diameter of the beam waist), the focus of the beam was observed whilst applying phase steps across the pulse using a CCD (LaserCam HR, Coherent, Inc.). It was found that the maximum deviation recorded was 0.8 μm. Considering that the $1/e^2$ diameter for the focused beam is 66 ± 3.3 μm, measured by the same CCD, the deviation measured can be attributed to the error of the measurement. Thus, it can be concluded that the phase step does not spatially move the focus point or affect the beam waist diameter.

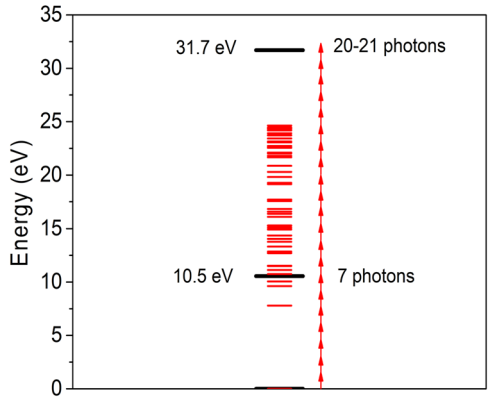

FIG. 2. The first and second ionization energies of methanol (black) with intermediate excited states (red).

QCC assumes resonant multiphoton transitions to excited states. We performed *ab initio* calculations to determine the states that would be accessible via multiphoton resonance for the given laser photon energy (1.550 eV) and bandwidth (0.0485 eV). The first and second ionization energies of methanol were obtained at the Coupled Cluster Single Double (Triple)/correlation consistent polarized Valence Double Zeta (CCSD(T)/cc-pVDZ) while using the ground state neutral structure geometry as obtained with CCSD/cc-pVDZ level of theory, this entitles our method as CCSD(T)/cc-pVDZ//CCSD/cc-pVDZ. Using the same geometry, excited states that would facilitate multiphoton resonance transitions were calculated at the equation-of-motion (EOM)-CCSD/cc-pVDZ level of theory. The results from these calculations are given in Fig. 2 and indicate a resonance at seven photons which coincides with the first ionization. Double ionization requires 20 or 21 photons; both values are possible because of the laser pulse bandwidth.

III. RESULTS

The experimental results obtained by scanning a π step across the spectrum of the laser while detecting different ions within the ToF mass spectrometer are shown in [Fig. 3(a)]. We observe that the ion yields of C^{2+} and H_3^+ behave as the theory predicts [see, for example, Fig. 1(c)], namely, their yields decrease as the phase step is swept across the spectrum, reaching a minimum near ω_o [Fig. 3(a)]. However, the yield of CHO^+ (or COH^+, indistinguishable by ToF) did not follow this pattern. In fact, some enhancement above the TL yield was observed. This significant deviation from theory occurs near the FWHM points in the spectrum. We scanned the magnitude of the phase step, increasing from 0 to 2π, while keeping the phase step positioned at the two FWHM points, one in the red region and one in the blue region of the spectrum. The experiments were carried out at three different laser intensities, and the results are summarized in Fig. 3(b). The relative difference in the H_3^+ yield, defined as the difference between the maximum yield in each region of the spectrum $I(\omega_b) - I(\omega_r)$

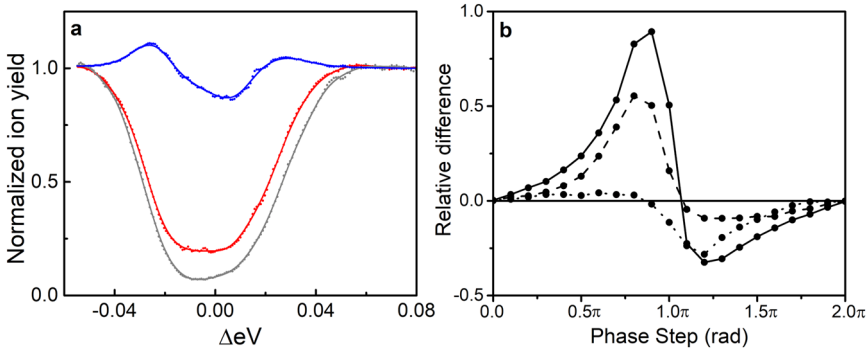

FIG. 3. (a) The yield of, CHO^+ (blue), H_3^+ (red), and C^{2+} (grey), detected as a function of scanning a π-step phase across the spectrum normalized to their value when TL pulses are used. Note that in general, the ion yield decreases; however, for CHO^+ we observe a relative increase above what is observed for TL pulses. (b) Relative difference in the yield of H_3^+ ions $(I(\omega_b) - I(\omega_r))/((I(\omega_b) + I(\omega_r))/2)$ at three different laser intensities; 5.5 (dashed line), 4.3 (solid line) and 3.8 (dotted line) $\times 10^{14}$ W/cm^2. Notice that significant changes are observed for non-integer values of π.

(where ω_r is the maximum yield in the red region and ω_b is the maximum yield in the blue region) divided by the average $((I(\omega_b) + I(\omega_r))/2)$ where $\omega_r = -0.012$ eV and $\omega_b = 0.018$ eV relative to ω_0, highlights that the ion yield is dependent on the position that the phase step is applied. We find that a π step makes little or no difference, but a positive or negative 3/4 π step across the spectrum results in the greatest relative difference, Fig. 3(b).

When sweeping positive or negative 3/4 π steps across the spectrum, we observe large deviations in the ion yields normalized to TL, when the step is near the FWHM of the pulse spectrum, that are not predicted by QCC; see Fig. 4(a). CHO^+ and H_3^+ ion yield enhancement occurs when a negative phase step is located in the low-energy portion of the spectrum and when a positive phase step is located in the high-energy region of the spectrum. The relative differences observed are calculated by $(\varphi_+ - \varphi_-)/((\varphi_+ + \varphi_-)/2)$ and are shown in Fig. 4(b). Near −0.01 eV, changing the sign of the phase step causes a factor of seven enhancement in the observed H_3^+ ion-yield.

We measured the yield of all ions as a function of linear and circular polarized light. It can be seen in Fig. 5 that the yield of ions C^{2+} and H_3^+ decreases when the polarization of light is changed from linear to circular. The molecular ion yield, CH_3OH^+, shows no dependence on the polarization of the light.

In order to rule out that the observed changes in ion yields shown in Fig. 4 depend only on peak intensity, we carried out measurements as a function of linear chirp (second order dispersion). The results, shown in Fig. 6, indicate that while the yield of the different ions depends on peak intensity, the ion yield decreases symmetrically, with H_3^+ decreasing more significantly than CHO^+. At 1000 fs^2, the effective chirp introduced by the phase step, there is almost no difference, ~0.75%, between the positive and negative chirp ion yields.

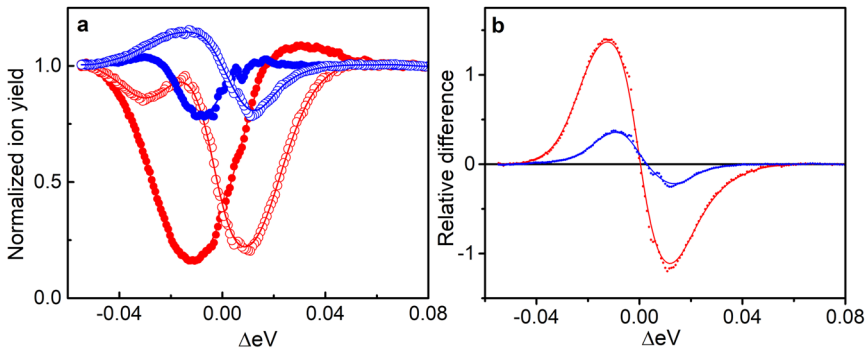

FIG. 4. (a) The yield of selected ions, H_3^+ (red) and CHO^+ (blue), detected as a function of scanning a ±3/4 π step phase, −3/4 π (hollow dots) and +3/4 π (filled dots), across the spectrum normalized to their value when TL pulses. In addition to the experimental points, we show a line resulting from 5-point smoothing. (b) Relative difference in the yield of H_3^+ (red) and CHO^+ (blue) ions calculated by $(\varphi_+ - \varphi_-)/((\varphi_+ + \varphi_-)/2)$.

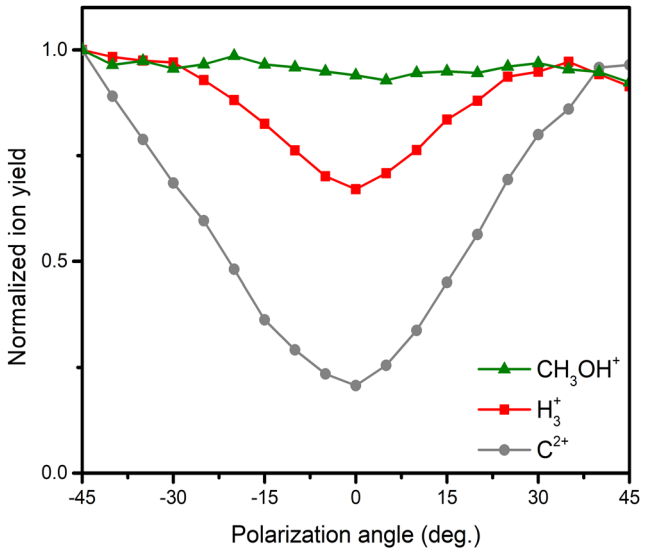

FIG. 5. Ion yield dependence on the angle of polarization of the light at 4.8×10^{14} W/cm^2. At 0°, the light is circularly polarized, and at ± 45°, it is linear (parallel to the ToF axis).

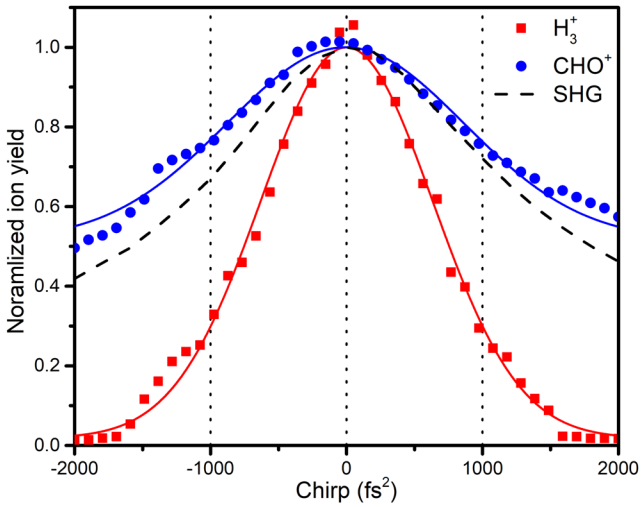

FIG. 6. Ion yield dependence on the amount of 2nd order dispersion (chirp) applied at a laser intensity of 4.8×10^{14} W/cm^2. H_3^+ is in red with square symbols, CHO^+ is in blue with circular symbols, and the black dashed line is the second-harmonic intensity dependence, included as a reference.

IV. DISCUSSION

The formation of H_3^+ requires double ionization, formation of neutral H_2, and the abstraction of a proton following roaming.[17] The first and second ionization energies for methanol require the absorption of 7 and 20 (~1.55 eV) photons, respectively, based on our calculations, under the experimental conditions (Fig. 2). At the peak laser intensity, when the pulses are transform limited, the Keldysh parameter is 0.45,[22] implying that single ionization occurs predominantly through a tunneling mechanism. Subsequently, double-ionization likely occurs through rescattering,[23,24] as confirmed by the observed H_3^+ yield decreasing when the polarization of the laser was changed from linear to circular (Fig. 5).[25] Following strong-field ionization, some electrons remain in a coherent superposition of excited states (or Rydberg states), which oscillate with frequencies that closely correspond to the harmonics of the laser.[26,27] These excited states are highly susceptible to further ionization depending on the properties of the pulse.

One would expect that if a π step was applied to a 20-photon absorption process, the peak intensity reduction alone would cause a major reduction in ion yield. This would result in a significant depletion of all ion yields that require a doubly charged parent ion, such as H_3^+. However, an overall depletion is not observed. Depending on the sign of π step, we observe either depletion or enhancement. This is in contrast to the prediction by QCC theory of an overall depletion that is symmetric about the center of the spectrum [see Fig. 1(b)].

The reader should note that a $\pm 3/4\ \pi$ step has an asymmetric effect on the electric field similar to that shown a $\pm\pi/2$ step [Fig. 1(d)]. When the step is positive, the pulse breaks into a weaker portion that is followed by a more intense pulse, and vice versa. Analysis of our data showed that enhancement is observed for negative phase steps in the red region (ω_r) and positive phase steps in the blue region (ω_b). This indicates that the temporal shape of the pulse $I(t)$, i.e., the order of these sub-pulses, cannot be responsible for the observed enhancement. Therefore, a more complete description of the pulses that includes the time-dependent phase $\Phi(t)$ and the instantaneous frequency of the pulse $\omega(t)$ were carried out and are shown in Fig. 7. A description of the pulses where the phase step is applied at ω_0 alongside the phase-space relationship (Wigner plot) of the pulses can be found in the supplementary material. From the analysis, we note that pulses that result in enhancement [Figs. 7(a) and 7(b)] are associated with a downchirp during the more intense part of the pulse, indicated by a straight line. Pulses that resulted in yield depletion [Figs. 7(c) and 7(d)] show an up-chirp in the portion of the pulse with greater intensity. Down-chirped pulses have been shown to increase vibrational excitation via intrapulse pump-dump processes similar to stimulated Raman scattering, increasing the ground state vibrational energy.[28–30] However, recall that we found no difference in the ion yields between positive or negative chirp (Fig. 6). This implies that the abrupt change in phase following the downchirp is essential for the observed strong-field QCC effects being reported here.

At this moment, it is unclear if the shaped pulses are controlling the rescattering process leading to double ionization, or if the additional vibrational energy from the pump-dump process controls the fragmentation. If we are controlling the rescattering process, then we would predict that phase step pulses should exert similar control over atomic double ionization, as well as the multiple processes associated with rescattering such as high harmonic generation.[23]

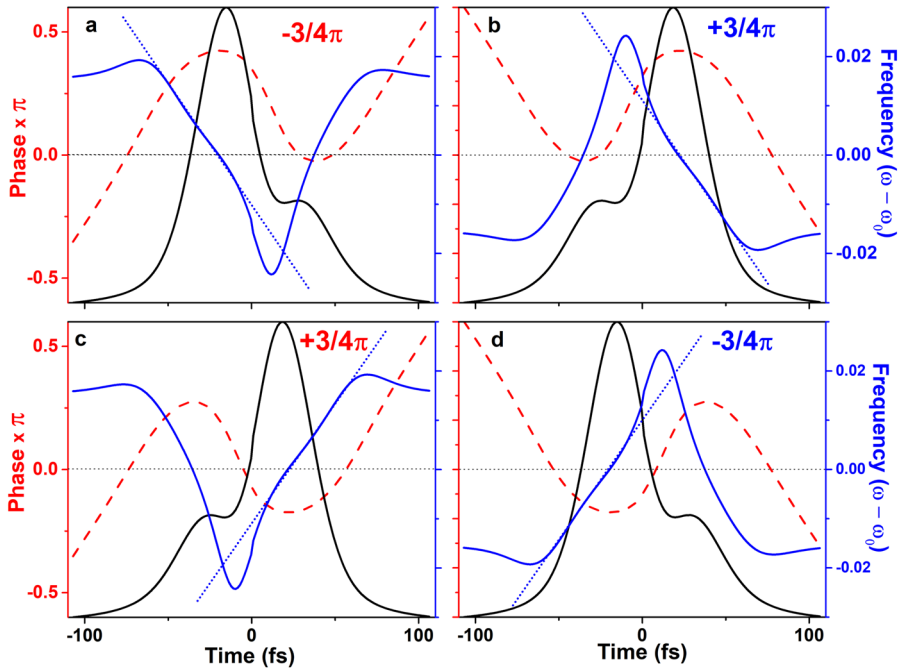

FIG. 7. The time-dependent intensity (black line) $I(t)$, phase (dashed red line) $\Phi(t)$, and the instantaneous frequency of the pulse (blue line) $\omega(t)$ for the two cases where enhancement was observed, (a) $(-3/4\pi\ \omega_r)$ and (b) $(+3/4\pi\ \omega_b)$ and where suppression was observed (c) $(+3/4\pi\ \omega_r)$ and (d) $(-3/4\pi\ \omega_b)$. When the phase step causes enhancement, a downchirp is observed in the most intense feature of the pulse and is indicated by a dotted line. When there is yield suppression, there is an up-chirp in the frequency. The time-dependent phase $\Phi(t)$ and the instantaneous frequency of the pulse $\omega(t)$ applied at ω_0 are shown in the supplementary material.

Proton migration has been recently controlled by the carrier envelope phase (CEP) of the incident strong field.[31] In that work, the vibrational wave packet formed by the pulse and double ionization were shown to depend CEP. Based on those observations, one would expect the downchirp in our experiments to induce molecular vibrations and the sudden change in phase to control the phase-dependent rescattering process. In future studies, we will investigate how the phase step pulses used here affect rescattering by looking at much simpler systems which can be supported by theory. Furthermore, we are planning to investigate if our observations are partly due to multiphoton resonances. In our experimental conditions, seven photons are required to singly ionize methanol. Experiments with different laser pulse wavelengths and on different compounds will help identify if electronic resonances are consistent with our experimental and theoretical observations.

V. CONCLUSION

To conclude, we have applied shaped pulses with π, and non-integer values of π, phase steps to explore quantum coherent control of H_3^+ yield following the strong laser field excitation of methanol. Our results show an unexpected seven-fold enhancement in the ion yield that at times exceeds that for transform-limited pulses. The enhancement is not predicted by perturbative QCC as derived for two- and three-photon excitation. Our experimental observation indicates strong field QCC on molecules that require multiphoton (>7) excitation is possible. However, it is clear that there are several complex processes occurring and the observed effects are not simply caused by a single variable such as the excitation frequency, the temporal intensity shape of the pulse, or the chirp. Therefore, we conclude that the observed control results from a combination of temporal, spectral, and phase effects. Roaming mechanisms such as those discussed here suggest molecules under Coulomb explosion conditions caused by strong fields do not behave as a "bag of atoms" and are controllable through pulse shaping. We are carrying out experiments on small molecules and in isolated atoms in order to determine the generality of our findings, and the dependence on molecular parameters.

SUPPLEMENTARY MATERIAL

Further details regarding the method can be found in the supplementary material alongside a fully annotated mass spectrum of methanol. A description of the pulses where the phase step is applied at ω_0 and the phase-space relationship (Wigner plot) of the pulses can also be found.

ACKNOWLEDGMENTS

This material is based upon work supported by the U.S. Department of Energy, Office of Science, Office of Basic Energy Sciences, Atomic, Molecular and Optical Sciences Program under Award No. SISGR (DE-SC0002325). The authors recognize the feedback received from Mr. Justin Rose during manuscript preparation.

REFERENCES

[1] D. Meshulach and Y. Silberberg, Nature **396**, 239 (1998).
[2] P. Brumer and M. Shapiro, Acc. Chem. Res. **22**, 407 (1989).
[3] R. Kosloff, S. A. Rice, P. Gaspard, S. Tersigni, and D. J. Tannor, Chem. Phys. **139**, 201 (1989).
[4] R. S. Judson and H. Rabitz, Phys. Rev. Lett. **68**, 1500 (1992).
[5] A. Gandman, L. Chuntonov, L. Rybak, and Z. Amitay, Phys. Rev. A **75**, 031401 (2007).
[6] A. Konar, V. V Lozovoy, and M. Dantus, J. Phys. Chem. A **120**, 2002 (2016).
[7] D. Meshulach and Y. Silberberg, Phys. Rev. A **60**, 1287 (1999).
[8] T. Seideman, M. Y. Ivanov, and P. B. Corkum, Phys. Rev. Lett. **75**, 2819 (1995).
[9] X. Zhu, V. V Lozovoy, J. D. Shah, and M. Dantus, J. Phys. Chem. A **115**, 1305 (2011).
[10] V. V. Lozovoy, T. C. Gunaratne, J. C. Shane, and M. Dantus, ChemPhysChem **7**, 2471 (2006).
[11] N. Dudovich, B. Dayan, S. M. Gallagher Faeder, and Y. Silberberg, Phys. Rev. Lett. **86**, 47 (2001).
[12] V. Blanchet, C. Nicole, M.-A. Bouchene, and B. Girard, Phys. Rev. Lett. **78**, 2716 (1997).
[13] B. Dayan, A. Pe'er, A. A. Friesem, and Y. Silberberg, Phys. Rev. Lett. **93**, 023005 (2004).
[14] J. H. D. Eland and B. J. Treves-Brown, Int. J. Mass Spectrom. Ion Processes **113**, 167 (1992).
[15] K. Hoshina, Y. Furukawa, T. Okino, and K. Yamanouchi, J. Chem. Phys. **129**, 104302 (2008).
[16] A. M. Mebel and A. D. Bandrauk, J. Chem. Phys. **129**, 224311 (2008).
[17] N. Ekanayake, M. Nairat, B. Kaderiya, P. Feizollah, B. Jochim, T. Severt, B. Berry, K. R. Pandiri, K. D. Carnes, S. Pathak, D. Rolles, A. Rudenko, I. Ben-Itzhak, C. A. Mancuso, B. S. Fales, J. E. Jackson, B. G. Levine, and M. Dantus, Sci. Rep. **7**, 4703 (2017).
[18] N. Ekanayake, T. Severt, M. Nairat, N. P. Weingartz, B. M. Farris, B. Kaderiya, P. Feizollah, B. Jochim, F. Ziaee, K. Borne, K. Raju P., K. D. Carnes, D. Rolles, A. Rudenko, B. G. Levine, J. E. Jackson, I. Ben-Itzhak, and M. Dantus, Nat. Commun. **9**, 5186 (2018).
[19] N. Ekanayake, M. Nairat, N. P. Weingartz, M. Michie, B. G. Levine, and M. Dantus, J. Chem. Phys. **149**, 244310 (2018).
[20] B. Xu, J. M. Gunn, J. M. Dela Cruz, V. V. Lozovoy, and M. Dantus, J. Opt. Soc. Am. B **23**, 750 (2006).
[21] Y. Coello, V. V. Lozovoy, T. C. Gunaratne, B. Xu, I. Borukhovich, C. Tseng, T. Weinacht, and M. Dantus, J. Opt. Soc. Am. B **25**, A140 (2008).
[22] L. V. Keldysh, J. Exp. Theor. Phys. **47**, 1945 (1965).
[23] P. B. Corkum, Phys. Rev. Lett. **71**, 1994 (1993).
[24] B. Walker, B. Sheehy, L. F. DiMauro, P. Agostini, K. J. Schafer, and K. C. Kulander, Phys. Rev. Lett. **73**, 1227 (1994).
[25] P. Dietrich, N. H. Burnett, M. Ivanov, and P. B. Corkum, Phys. Rev. A **50**, R3585 (1994).
[26] S. Chelkowski, T. Bredtmann, and A. D. Bandrauk, Phys. Rev. A **85**, 033404 (2012).
[27] G. K. Paramonov, O. Kühn, and A. D. Bandrauk, Mol. Phys. **115**, 1846 (2017).
[28] K. Duppen and D. A. Wiersma, Opt. Lett. **13**, 318 (1988).
[29] E. J. Brown, I. Pastirk, B. I. Grimberg, V. V. Lozovoy, and M. Dantus, J. Chem. Phys. **111**, 3779 (1999).
[30] J. Cao, C. J. Bardeen, and K. R. Wilson, J. Chem. Phys. **113**, 1898 (2000).
[31] M. Kübel, R. Siemering, C. Burger, N. G. Kling, H. Li, A. S. Alnaser, B. Bergues, S. Zherebtsov, A. M. Azzeer, I. Ben-Itzhak, R. Moshammer, R. de Vivie-Riedle, and M. F. Kling, Phys. Rev. Lett. **116**, 193001 (2016).